

Enlargement of optical Schrödinger's cat states

Demid V. Sychev^{1,2†}, Alexander E. Ulanov^{1,3†}, Anastasia A. Pushkina^{1,4}, Matthew W. Richards⁴, Ilya A. Fedorov^{1,5†} and Alexander I. Lvovsky^{1,4,5,6*}

Superpositions of macroscopically distinct quantum states, introduced in Schrödinger's famous Gedankenexperiment, are an epitome of quantum 'strangeness' and a natural tool for determining the validity limits of quantum physics. The optical incarnation of Schrödinger's cat (SC)—the superposition of two opposite-amplitude coherent states—is also the backbone of continuous-variable quantum information processing. However, the existing preparation methods limit the amplitudes of the component coherent states, which curtails the state's usefulness for fundamental and practical applications. Here, we convert a pair of negative squeezed SC states of amplitude 1.15 to a single positive SC state of amplitude 1.85 with a success probability of ~0.2. The protocol consists in bringing the initial states into interference on a beamsplitter and a subsequent heralding quadrature measurement in one of the output channels. Our technique can be realized iteratively, so arbitrarily high amplitudes can, in principle, be reached.

In Schrödinger's proposal, the life and death of a cat are entangled with the state of a decaying atom, which results in a macroscopic quantum-superposition state¹. This setting, originally used as a metaphor to demonstrate the absurdity of the newborn quantum theory in the macroscopic domain, remained a matter of thought experiment for about 50 years. As quantum physics matured, this paradox was revisited; nowadays, Schrödinger's cat (SC) is being emulated in diverse physical systems. It is expected to help answer a fundamental question^{2–4}: at what degree of macroscopicity, if any, does the world stop being quantum?

In optics, the SC state corresponds to a superposition of coherent states $|\pm\alpha\rangle$, which are considered the most classical of all states of light⁵. In such a superposition, the fields of the electromagnetic wave point in two opposite directions at the same time, which resembles the superposition of dead and alive states of a cat in the original concept. The size parameter in this case is the amplitude α . For the SC to be macroscopic, α has to be much larger than the quantum uncertainty $1/\sqrt{2}$ of the position observable in the coherent state^{5–7}.

Aside from the fundamental interest, optical SC states are useful in applied quantum science. They can serve as a basis for quantum computation^{8,9}, metrology^{10,11}, teleportation and cryptography^{12–14}. Most of these applications require the involved coherent states to be of reasonably high amplitudes. For example, encoding a qubit in the coherent state basis $|\pm\alpha\rangle$ is practical only when these states are nearly orthogonal, that is, when $\alpha \geq 2$ (ref. 8). Although a fault-tolerant quantum computation scheme optimized at $\alpha \approx 1.6$ has been proposed, it requires a significant resource overhead⁹.

The above motivation to build optical SC states inspired a significant experimental drive^{15–27}. Most of the existing experiments are based on photon subtraction from the squeezed vacuum state^{19–25} or on quantum-state engineering within the subspace of three lower Fock states^{15–18}. The state obtained by these methods approximates SCs reasonably well only for relatively small amplitudes. A better performance is offered by the method of preparing SCs from multiphoton Fock states²⁶, but these states are, themselves, difficult to prepare in a reliable and scalable fashion.

In this work, we implement an alternative for the direct-preparation approach mentioned above. Our technique probabilistically converts a pair of SCs into a single SC state with an amplitude greater than that of the initial ones by a factor of $\sqrt{2}$. Our method can be applied in an iterative manner^{27,28}, which allows one to prepare an SC state of, in principle, any desirable amplitude—given that sufficiently many initial SCs are available at the inception stage.

The idea of the method was proposed by Lund *et al.*²⁹ and further developed by Laghaout *et al.*²⁸. Let the initial SC state be a superposition of coherent states of real amplitude α be:

$$|SC_+[\alpha]\rangle = N(|\alpha\rangle + |-\alpha\rangle) \quad (1a)$$

$$|SC_-[\alpha]\rangle = N(|\alpha\rangle - |-\alpha\rangle) \quad (1b)$$

where N is the normalization factor. Suppose a pair of identical, either positive or negative, states (equation (1)) is put to interference on a symmetric beamsplitter. Let the relative phase of the inputs be such that equal coherent states interfere constructively in its output mode 1 and destructively in mode 2, whereas opposite-amplitude coherent states behave in the converse fashion. The two-mode output state of the beam splitter is then²⁹:

$$|\Psi\rangle_{12} = N\left(|SC_+[\sqrt{2}\alpha]\rangle_1|0\rangle_2 \pm |0\rangle_1|SC_+[\sqrt{2}\alpha]\rangle_2\right) \quad (2)$$

where $|0\rangle$ is the vacuum state. If we now perform a measurement on mode 2 to distinguish the states $|0\rangle$ and $|SC_+[\sqrt{2}\alpha]\rangle$, and detect the vacuum state, mode 1 will collapse onto the positive SC state of amplitude $\sqrt{2}\alpha$ (ref. 29).

The required conditioning can be realized by homodyne measurement of the position quadrature in mode 2 and looking for the null result. Indeed, the wavefunction of state $|SC_+[\sqrt{2}\alpha]\rangle_2$ is a sum of two Gaussians of width $1/\sqrt{2}$ centred, respectively, at $X = \pm\alpha\sqrt{2}$, whereas the wavefunction of the vacuum state is the same Gaussian centred at $X = 0$. Therefore, for $\alpha \gg 1$, the

¹International Center for Quantum Optics and Quantum Technologies (Russian Quantum Center), Skolkovo, Moscow 143025, Russia. ²Moscow State Pedagogical University, Department of Theoretical Physics, M. Pirogovskaya Str. 29, Moscow 119991 Russia. ³Moscow Institute of Physics and Technology, 141700 Dolgoprudny, Russia. ⁴Institute for Quantum Science and Technology, University of Calgary, Calgary, Alberta T2N 1N4, Canada. ⁵P. N. Lebedev Physics Institute, Leninsky Prospect 53, Moscow 119991, Russia. ⁶Canadian Institute for Advanced Research, 661 University Avenue, Toronto, Ontario M5G 1M1, Canada. [†]These authors contributed equally to the work. *e-mail: LVOV@ucalgary.ca

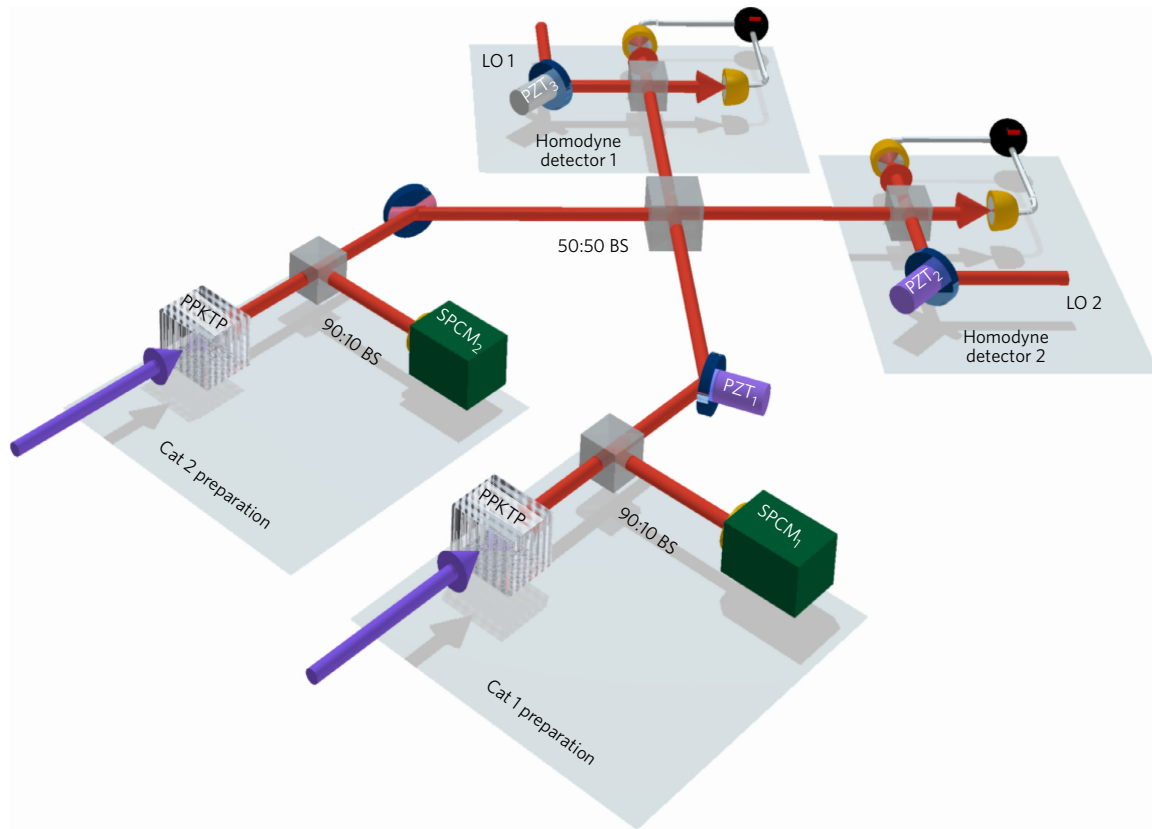


Figure 1 | Scheme of the experiment. A squeezed vacuum state is generated in each input channel via degenerate parametric downconversion (PPKTP). A small portion of the photon flux from each squeezer is directed to a SPCM; preparation of the two initial negative SC states is heralded by simultaneous clicks of SPCMs 1 and 2. The resulting SC states interfere on a 50:50 beamsplitter (BS). Optical homodyne tomography of the state in output mode 1 of the BS is performed, conditioned on the near-zero result of the position quadrature measurement in output mode 2. LO, local oscillator; PZT, piezoelectric transducer.

probability of observing $X=0$ is much higher in the vacuum state than in the state $|SC_+[\sqrt{2}\alpha]\rangle$. A precise calculation yields:

$$\begin{aligned} |\psi\rangle_1 &= {}_2\langle X=0|\psi\rangle_{12} \\ &= N \left(|SC_+[\sqrt{2}\alpha]\rangle_1 \pm \frac{|0\rangle_1}{\sqrt{(1+e^{4\alpha^2})/2}} \right) \end{aligned} \quad (3)$$

For the initial SC amplitude $\alpha = 1$, which is easily attained by present technology^{15,16,19,23–27}, state (3) has a fidelity of 99% with the ideal $|SC_+[\sqrt{2}]\rangle_1$ state²⁸ (throughout this paper, the fidelity between the states with density operators ρ_1 and ρ_2 is defined as $F = \text{Tr}[(\sqrt{\rho_1}\rho_2\sqrt{\rho_1})^{1/2}]$).

In experimental practice, the SC amplification event is heralded by observing X within a finite near-zero interval. In our case of $\alpha = 1.15$, we set the boundaries of this interval at 0.3, which gives a success probability of $p \approx 0.2$ without significant additional fidelity loss. Remarkably, the acceptable width of this interval and, consequently, the success probability of this protocol increases with α , reaching $p \approx 1/2$ for $\alpha \geq 2$. This is because the peaks in the wavefunction of the SC move further away from $X = 0$. Moreover, the fidelity of amplification also increases with α due to the diminishing weight of the vacuum component in equation (3).

The experimental set-up for realizing the above protocol is shown in Fig. 1. The initial SCs in two spatially distinct light modes are generated by photon subtraction from squeezed vacuum states^{19,30}. As the squeezed vacuum is approximated by

positive SC (equation (1a)), the photon annihilation flips the sign in front of the $|\alpha\rangle$ component, which converts the state to a negative squeezed SC (equation (1b)) of a larger amplitude^{19,20}. The obtained states are characterized by optical homodyne tomography^{31,32}. Corrected for the total quantum efficiency of 62% (Methods), they have a fidelity of 84% with an ideal state $|SC_-[1.15]\rangle$ squeezed by 1.74 dB. The Wigner functions of the experimentally reconstructed states and the best-fit state are shown in Fig. 2 (right column). Throughout this paper, we follow the concept of Ourjoumtsev *et al.*²⁶ by fitting our experimentally acquired states with squeezed SCs. The rationale behind this convention is that squeezing does not affect the macroscopicity of the superposition³³ and can be undone by a local unitary operation.

Simultaneous preparation of the two initial SC states is heralded by coincident clicks of single-photon counting modules (SPCMs) 1 and 2. The states are then mixed on a symmetric beamsplitter. The optical phase difference between them is stabilized actively (Methods) to make sure that the output state of the beamsplitter is described by equation (2). Subsequently, one of the beamsplitter output modes (mode 2) is subjected to homodyne measurement of the position quadrature. Conditioned on a near-zero measurement result ($|X| \leq 0.3$) in mode 2, the state of mode 1 is subjected to quantum tomography by means of another homodyne detector. Out of a total of 40,000 SPCM coincidence events collected, 8,000 satisfied this condition, which corresponds to the protocol's success probability of $p = 0.2$.

The tomographic reconstruction result is shown in Fig. 2a (right). The amplified state, corrected for a 62% detection efficiency, has a fidelity of 77% with $|SC_+[1.85]\rangle$ squeezed by 3.04 dB, displayed

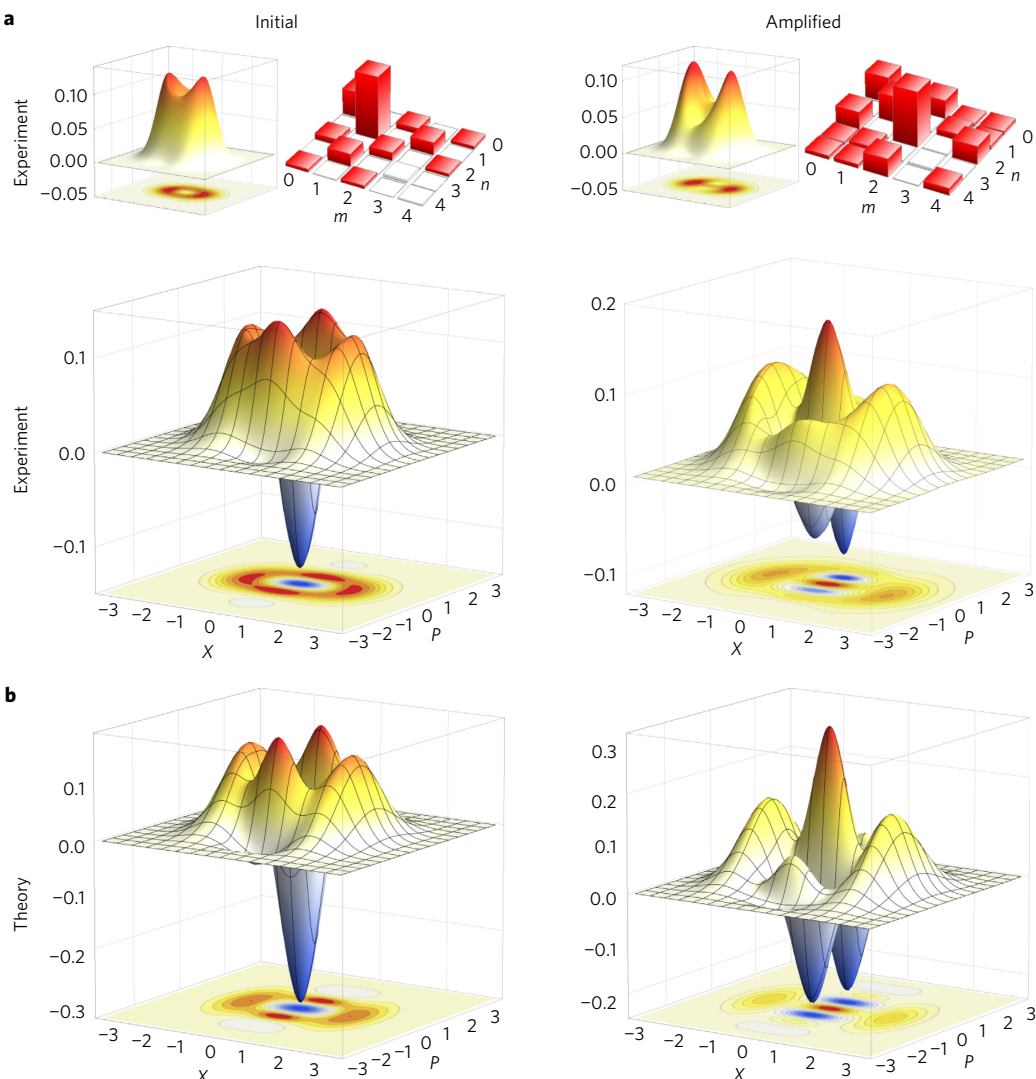


Figure 2 | Wigner functions of the initial and amplified SC states. **a**, Experimental reconstruction via homodyne tomography corrected for the total quantum efficiency of 62%. Left insets: Wigner functions reconstructed without efficiency corrections. X and P denote the position and momentum quadratures, respectively. Right insets: absolute values of density matrices ρ_{mn} in the Fock basis reconstructed with efficiency correction. **b**, Best fit with the ideal squeezed SC state. Left (right): initial (amplified) SC state. The best-fit state is $|\text{SC}_-[1.15]\rangle$ ($|\text{SC}_+[1.85]\rangle$) squeezed by 1.74 dB (3.04 dB). The fidelity between the theoretical and experimental (corrected) states is 84% (77%).

in Fig. 2b (right). The additional squeezing of the output SC compared with the input is a result of the non-ideality of the homodyne detection in mode 2 as well as the imperfection of the initial SC.

The Wigner functions of the SC states have a characteristic shape that consists of two positive Gaussian peaks associated with the individual coherent state constituents and a highly non-classical ‘interference fringe’ pattern between them. Our observations are consistent with this description. In the initial SC states, the Gaussian peaks are quite close to each other, so the Wigner function of the initial state resembles that of the squeezed single photon¹⁹. For the amplified SC, the peaks are separated further, so one can more clearly distinguish them from the interference pattern in between, with the latter becoming more prominent. This effect on the Wigner function is also quite evident without the efficiency correction (Fig. 2a, left insets).

The protocol demonstrated here constitutes an instrument to convert a pair of SC states into a single larger-amplitude positive SC state. The probability of success p is directly related to the width of the quadrature selection band in output mode 2 of the

beamsplitter, and asymptotically increases to 1/2 for high amplitudes. As shown, the fidelity of the amplified SC does not significantly decrease with respect to that of the initial one, which permits the application of the protocol in an iterative fashion.

A single realization of our protocol produces optical SCs with amplitudes that are comparable to the highest ever achieved, including other physical systems, such as microwave³⁴ and circuit³⁵ cavity quantum electrodynamics settings. Iterating our protocol for n stages will further increase the SC amplitude by a factor of $\alpha'/\alpha = 2^{n/2}$. As each implementation of the protocol would require two input SCs, a total of $1 + 2 + \dots + 2^{n-1} = 2^n - 1$ implementations are needed for n stages, with the corresponding success probability of $p^{2^{n-1}} = p^{-(\alpha'/\alpha)^{2-1}}$. This estimate can be increased by using wider acceptance intervals at advanced stages of the protocol with $\alpha \geq 2$. For example, amplifying the SC state from $\alpha = 1.4$ to $\alpha' = 4$ would require, on average, $\sim 5,000$ copies of the initial SC per one copy of the output.

The multistage version of the breeding protocol would function best with on-demand SC sources. The recently developed high-efficiency, reproducible single-photon sources^{36,37} are promising in

this context. The photons obtained from these sources can be subjected to squeezing to generate low-amplitude SCs, or used directly as the input states of the first stage²⁷. Alternatively, one can use heralded SC sources, such as those employed in this experiment, combined with optical quantum memory in a setting similar to the quantum repeater³⁸. This will change the scaling of the overall success probability with respect to the target amplitude from exponential to polynomial.

It is instructive to compare our method with the techniques for the heralded preparation of arbitrary Fock-state superpositions by engineering the measurement in the idler channel of parametric downconversion^{17,18}. Theoretically, any quantum state, including SCs, can be decomposed into the Fock basis and thus prepared in this fashion. In practice, however, these methods operate in the limit of low probability to generate a photon pair. Hence, in contrast to the method developed here, they feature prohibitively low success probabilities for any states beyond the 2–3 photon subspace.

Methods

Methods and any associated references are available in the [online version of the paper](#).

Received 3 November 2016; accepted 17 March 2017;

published online 1 May 2017

References

- Schrödinger, E. *Die gegenwärtige situation in der quantenmechanik. Naturwissenschaften* **23**, 807–812 (1935).
- Haroche, S. Nobel lecture: controlling photons in a box and exploring the quantum to classical boundary. *Rev. Mod. Phys.* **85**, 1083–1102 (2013).
- Wineland, D. J. Nobel lecture: superposition, entanglement, and raising Schrödinger's cat. *Rev. Mod. Phys.* **85**, 1103–1114 (2013).
- Markus, A. & Hornberger, K. Testing the limits of quantum mechanical superpositions. *Nat. Phys.* **10**, 271–277 (2014).
- Leonhardt, U. *Measuring Quantum States of Light* (Cambridge Univ. Press, 1997).
- Leggett, A. J. Testing the limits of quantum mechanics: motivation, state of play, prospects. *J. Phys. Condens. Matter* **14**, R415–R451 (2002).
- Lvovsky, A. I., Ghobadi, R., Chandra, A., Prasad, A. S. & Simon, C. Observation of micro–macro entanglement of light. *Nat. Phys.* **9**, 541–544 (2013).
- Ralph, T. C., Gilchrist, A., Milburn, G. J., Munro, W. J. & Glancy, S. Quantum computation with optical coherent states. *Phys. Rev. A* **68**, 042319 (2003).
- Lund, A. P., Ralph, T. C. & Haselgrove, H. L. Fault-tolerant linear optical quantum computing with small-amplitude coherent states. *Phys. Rev. Lett.* **100**, 030503 (2007).
- Joo, J., Munro, W. J. & Spiller, T. P. Quantum metrology with entangled coherent states. *Phys. Rev. Lett.* **107**, 083601 (2011).
- Facon, A. et al. A sensitive electrometer based on a Rydberg atom in a Schrödinger-cat state. *Nature* **535**, 262–265 (2016).
- Lee, S.-W. & Jeong, H. Near-deterministic quantum teleportation and resource-efficient quantum computation using linear optics and hybrid qubits. *Phys. Rev. Lett.* **87**, 022326 (2012).
- Sangouard, N. et al. Quantum repeaters with entangled coherent states. *J. Opt. Soc. Am. B* **27**, A137–A145 (2010).
- Brask, J. B., Rigas, I., Polzik, E. S., Andersen, U. L. & Sørensen, A. S. Hybrid long-distance entanglement distribution protocol. *Phys. Rev. Lett.* **105**, 160501 (2010).
- Huang, K. et al. Optical synthesis of large-amplitude squeezed coherent-state superpositions with minimal resource. *Phys. Rev. Lett.* **115**, 023602 (2015).
- Ulanov, A. E., Fedorov, I. A., Sychev, D., Grangier, P. & Lvovsky, A. I. Loss-tolerant state engineering for quantum-enhanced metrology via the reverse Hong–Ou–Mandel effect. *Nat. Commun.* **7**, 11925 (2016).
- Bimbard, E., Jain, N., MacRae, A. & Lvovsky, A. I. Quantum-optical state engineering up to the two-photon level. *Nat. Photon.* **4**, 243–247 (2010).
- Yukawa, M. et al. Generating superposition of up-to three photons for continuous variable quantum information processing. *Opt. Express* **21**, 5529–5535 (2013).
- Ourjoumtsev, A., Tualle-Brouri, R., Laurat, J. & Grangier, P. Generating optical Schrödinger kittens for quantum information processing. *Science* **312**, 83–86 (2006).
- Neergaard-Nielsen, J. S., Melholt Nielsen, B., Hettich, C., Mølmer, K. & Polzik, E. S. Generation of a superposition of odd photon number states for quantum information networks. *Phys. Rev. Lett.* **97**, 083604 (2006).
- Wakui, K., Takahashi, H., Furusawa, A. & Sasaki, M. Photon subtracted squeezed states generated with periodically poled KTiOPO₄. *Opt. Express* **15**, 3568–3574 (2007).
- Ourjoumtsev, A., Ferreyrol, F., Tualle-Brouri, R. & Grangier, P. Preparation of non-local superpositions of quasi-classical light states. *Nat. Phys.* **5**, 189–192 (2009).
- Gerrits, T. et al. Generation of optical coherent state superpositions by number-resolved photon subtraction from squeezed vacuum. *Phys. Rev. A* **82**, 031802(R) (2010).
- Takahashi, H. et al. Generation of large-amplitude coherent-state superposition via ancilla-assisted photon subtraction. *Phys. Rev. Lett.* **101**, 233605 (2008).
- Dong, R. et al. Generation of picosecond pulsed coherent state superpositions. *J. Opt. Soc. Am. B* **31**, 1192–1201 (2014).
- Ourjoumtsev, A., Jeong, H., Tualle-Brouri, R. & Grangier, P. Generation of optical Schrödinger cats from photon number states. *Nature* **448**, 1784–1786 (2007).
- Etesse, J., Bouillard, M., Kanseri, B. & Tualle-Brouri, R. Experimental generation of squeezed cat states with an operation allowing iterative growth. *Phys. Rev. Lett.* **114**, 193602 (2015).
- Laghaout, A. et al. Amplification of realistic Schrödinger-cat-state-like states by homodyne heralding. *Phys. Rev. A* **87**, 043826 (2013).
- Lund, A. P., Jeong, H., Ralph, T. C. & Kim, M. S. Conditional production of superpositions of coherent states with inefficient photon detection. *Phys. Rev. A* **70**, 020101 (2004).
- Dakna, M., Anhut, T., Opatrný, T., Knöll, L. & Welsch, D.-G. Generating Schrödinger-cat-like states by means of conditional measurements on a beam splitter. *Phys. Rev. A* **55**, 3184–3194 (1997).
- Lvovsky, A. I. & Raymer, M. G. Continuous-variable optical quantum-state tomography. *Rev. Mod. Phys.* **81**, 299–332 (2009).
- Lvovsky, A. I. Iterative maximum-likelihood reconstruction in quantum homodyne tomography. *J. Opt. B* **6**, S556–S559 (2004).
- Lee, C. W. & Jeong, H. Quantification of macroscopic quantum superpositions within phase space. *Phys. Rev. Lett.* **106**, 220401 (2011).
- Deléglis, S. et al. Reconstruction of non-classical cavity field states with snapshots of their decoherence. *Nature* **455**, 510–515 (2008).
- Vlastakis, B. et al. Deterministically encoding quantum information using 100-photon Schrödinger cat states. *Science* **342**, 607–610 (2013).
- Ding, X. et al. On-demand single photons with high extraction efficiency and near-unity indistinguishability from a resonantly driven quantum dot in a micropillar. *Phys. Rev. Lett.* **116**, 020401 (2016).
- Somashi, N. et al. Near-optimal single-photon sources in the solid state. *Nat. Photon.* **10**, 340–345 (2016).
- Lvovsky, A. I., Sanders, B. C. & Tittel, W. Optical quantum memory. *Nat. Photon.* **3**, 706–714 (2009).

Acknowledgements

We thank Y. Kurochkin and A. Turlapov for discussions. We acknowledge financial support from the Ministry of Education and Science of the Russian Federation (Agreement 14.582.21.0009, ID RFMEFI58215X0009). A.I.L. is supported by the Natural Sciences and Engineering Research Council of Canada and is a Canadian Institute for Advanced Research Fellow.

Author contributions

All the authors participated in the conception and planning of the project, theoretical analysis and writing of the paper. The experiment was performed by D.V.S., A.E.U., A.A.P., I.A.F. and M.W.R. The data were analysed by D.V.S., A.E.U., I.A.F. and A.I.L.

Additional information

Reprints and permissions information is available online at [www.nature.com/reprints](#).

Publisher's note: Springer Nature remains neutral with regard to jurisdictional claims in published maps and institutional affiliations. Correspondence and requests for materials should be addressed to A.I.L.

Competing financial interests

The authors declare no competing financial interests.

Methods

Degenerate parametric downconversion takes place in periodically poled potassium titanyl phosphate crystals (PPKTP, Raicol) under type-I phase-matching conditions. Each of the two crystals is pumped with ~ 25 mW frequency-doubled radiation of the master laser (Ti:Sapphire Coherent Mira 900D, with a wavelength of 780 nm, repetition rate of 76 MHz and pulse width of ~ 1.5 ps). In each nonlinear crystal, a 1.7 dB single-mode squeezed vacuum state is generated³⁹.

For the preparation of the initial SCs, 10% of the energy from these squeezed vacuum states is ‘tapped’ by beam splitters and directed to SPCMs (Excellitas) via fibre interfaces. The preparation rate of each SC state is ~ 10 kHz, which results in a ~ 2 Hz rate of coincidence events.

The set-up requires two phase-lock loops (PLLs), one to keep the input SCs in phase with each other and the other to ensure that the homodyne detector in mode 2 measures the X quadrature. To generate the feedback signal, both PLLs use the data from the homodyne detectors without conditioning on the SPCM events (which we refer to as ‘non-triggered’). The first PLL is set to minimize the Einstein–Podolsky–Rosen-type quadrature correlations, which show up in the detectors’ measurements when the phases are misaligned³⁹. The feedback signal is applied to a piezoelectric transducer in one of the initial state’s paths (PZT₁ in Fig. 1).

If the first PLL functions properly, the non-triggered output of the beam splitter constitutes two unentangled single-mode momentum-squeezed states. The second PLL can therefore be set to keep the variance of the mode 2 quadrature measurements at the maximum. The feedback signal is applied to the corresponding local oscillator phase via PZT₂ (Fig. 1).

The reconstruction of both the initial and amplified SC states is performed using the iterative maximum-likelihood algorithm^{31,32}. The local oscillator phase is varied by PZT₃ and its time-dependent value is extracted from the variance of the non-triggered quadrature data, which corresponds to the single-mode squeezed state. To perform the tomography of the initial SCs, the reflectivity of the central beam splitter is set to zero.

The total quantum efficiency of state detection, 62%, is determined from the analysis of these SC states⁴⁰. The main efficiency reduction factors are optical losses

(10%, not counting the tapping beam splitter), mode matching between the signal and local oscillator (81%) and the efficiency of the homodyne detector⁴¹ (86%).

The observed experimental imperfections can be explained by the model of Ourjoumtsev *et al.*¹⁹. According to this model, the SPCMs’ dark events, as well as imperfect matching between the modes detected by the SPCMs and the squeezed mode, results in an imperfect photon subtraction. The density matrix of the input SC is thus given by $\hat{\rho}_- = \xi |SC_-[\alpha]\rangle\langle SC_-[\alpha]| + (1 - \xi)\rho_{sq}$, where ρ_{sq} is the density matrix of the squeezed vacuum state subjected to 10% of losses on the tapping beam splitter. The best fidelity of 98% between the model and the experimentally reconstructed state was found for $\xi = 0.9$.

Subsequently, the ‘breeding’ protocol was applied to the modelled input SC, taking into account the efficiency of the heralding homodyne detector. The best fit gives a 97% fidelity with the experimentally obtained density matrix.

If the parameter ξ was equal to 0.99 and the tapping beam splitter reflectivity was 0.05 rather than 0.1, which can be achieved by modern experimental methods, the fidelity between the ideal cat states and the output (input) states calculated using the same model would be 95% (96%). In other words, the fidelity loss observed for the amplified SC in the present experiment mainly results from the imperfections in the initial SC rather than the ‘breeding’ operation itself.

Data availability. The data that support the plots within this paper and other findings of this study are available from the corresponding author on reasonable request.

References

39. Fedorov, I. A., Ulanov, A. E., Kurochkin, Y. & Lvovsky, A. I. Synthesis of the Einstein–Podolsky–Rosen entanglement in a sequence of two single-mode squeezers. *Opt. Lett.* **42**, 132–134 (2017).
40. Berry, D. W. & Lvovsky, A. I. Linear-optical processing cannot increase photon efficiency. *Phys. Rev. Lett.* **105**, 203601 (2010).
41. Kumar, R. *et al.* Versatile wideband balanced detector for quantum optical homodyne tomography. *Opt. Commun.* **285**, 5259–5267 (2012).